Supporting Information

Chemical requirement for extracting energetic charge carriers from plasmonic metal nanoparticles to perform electron-transfer reactions

Vishal Govind Rao, Umar Aslam, and Suljo Linic*

Department of Chemical Engineering, University of Michigan, Ann Arbor, Michigan 48109, USA.

* E-mail: linic@umich.edu

Nanoparticle synthesis, characterization and sample preparation for Raman measurement:

The silver nanocubes were synthesized using a polyol method as reported previously.[1] In brief, 10 mL of ethylene glycol were preheated at 140 °C for 1 h. Then 80 μL of 36 mM HCl were introduced to the mixture followed by the addition of 5 mL of a 10 mg/mL solution of polyvinylpyrrolidone (PVP, MW=55,000 Sigma Aldrich) in ethylene glycol. Next 2 mL of a 25 mg/mL solution of $AgNO_3$ (Acros Organics, ultrapure grade 99.5%) were added and a ventilated cap was positioned on the reaction vessel. After allowing the reaction mixture to sit overnight, the ventilated cap was replaced with an air-tight cap. The mixture was allowed to react for ~7 hours to form the Ag nanocubes. To wash the particles, the sample was diluted to 45 mL with water and centrifuged for 20 minutes at 8,000 rpm. The supernatant was disposed and the nanocubes were resuspended in 5 mL of DI water. This washing procedure was repeated twice and the resulting nanoparticles were redispersed in 10 mL of DI water.

The Ag-Pt core-shell nanocubes were synthesized using a recently published method.[2] A sample of purified Ag nanocubes in 10 mL of DI water was added to a Teflon beaker. Then 200 mg of PVP was dissolved in the reaction mixture. The Pt precursor solution was made by adding 32 mg of K_2PtCl_4 (Sigma Aldrich, 99.99%) in 5 mL of DI water. The pH of this solution was adjusted to ~12 by adding 50 μL of a 1.25 M aqueous NaOH solution. To prepare the reducing solution, 250 mg of ascorbic acid were dissolved in 3.5 mL of DI water. The pH of this mixture was increased to ~12 by adding 1.5 mL of a 1.25 M NaOH solution. This reducing solution was then added to the reaction mixture under stirring followed by the addition of the Pt precursor solution. Every hour, 100 μL of 1.25 M NaOH were added to the reaction mixture to maintain a high pH. The mixture was allowed to react for 2 hours and then promptly washed via centrifugation by diluting to 45 mL basic (~12 pH) DI water, and centrifuged for 20 minutes at 10,000 rpm. After discarding the supernatant, the nanoparticles were washed once more.

After the synthesis of Ag and core–shell Ag–Pt nanoparticles, the aqueous colloidal suspension and the aggregates on a solid substrate were characterized by UV−vis spectrophotometry (Thermo Evolution 300). The LSPR peak of Ag–Pt NC showed a red shift together with drop in intensity and broadening of the plasmon resonance than Ag nanoparticle (Figure S1). This is consistent with prior literature reports and can be accounted for by considering decay of plasmon resonance

into electron-hole pair via scattering at the metal/metal interface and the difference in frequency dependence of Ag and Pt dielectric constants.[3,4]

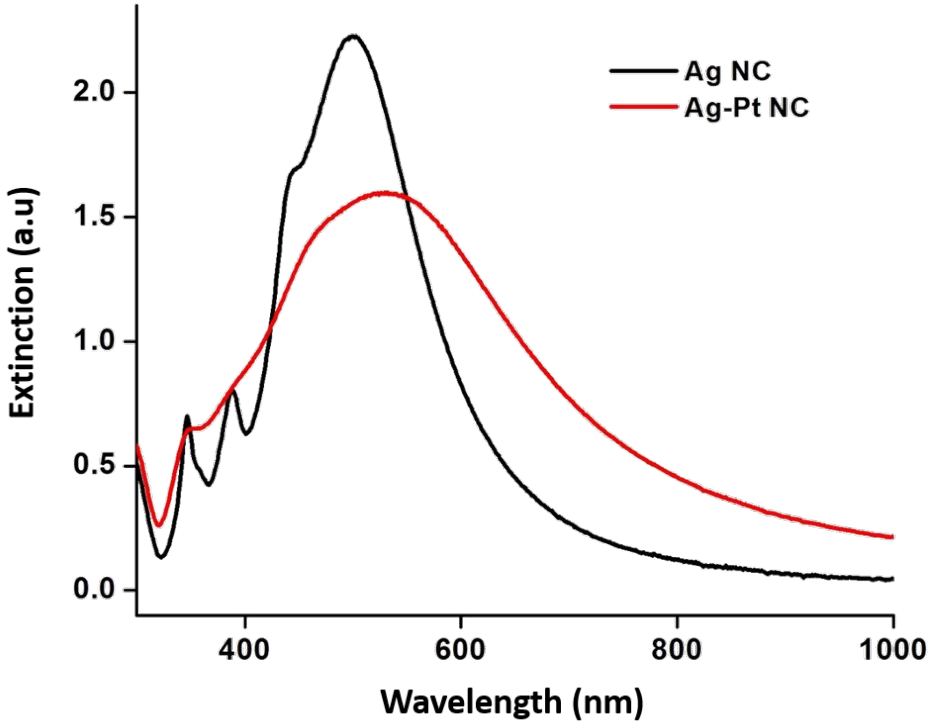

Figure S1: UV-vis extinction spectra of Ag NC and core–shell Ag–Pt NC in water.

The Ag and Ag–Pt dry aggregated samples for extinction measurements were prepared by drop-casting ~400 μL of the colloidal solution onto a glass slide and allowing the solvent to evaporate at ~323 K. Figure S2 shows the extinction spectra of both Ag and core–shell Ag–Pt nanoparticle in water and on glass. Because of the random nature of the Ag and Ag–Pt nanocube aggregates used in our studies (Figure S3 show TEM image of Ag and Ag–Pt nanocube aggregates), there are many different nanoparticle orientations and separation distances. These geometries lead to a broad range of coupled plasmon resonances at longer photon wavelengths. This manifests itself in the optical extinction data as a broad extinction feature from 600 to 900 nm for Ag nanocubes (Figure S2 (a), red spectrum) and almost flat extinction feature from 450 to 900 nm for Ag–Pt nanocubes (Figure S2 (b), red spectrum). Therefore, due to the random nature of the nanoparticle clustering

in our system, we expect that there are different spots that support plasmon resonance peaks over a broad range of wavelengths including 532 and 785 nm.

STEM samples were prepared by drop-casting a small amount of the colloidal nanoparticles onto 200 mesh copper grids. Aberration-corrected STEM (JEOL 3100, accelerating voltage 300 kV) was used to characterize the Ag and Ag–Pt nanocubes. The Ag cubes were found to have an average edge length of 65 ± 10 nm and in the Ag–Pt nanocubes the thickness of Pt shell were found to have an average length of ~1.2 nm (Figure S3).

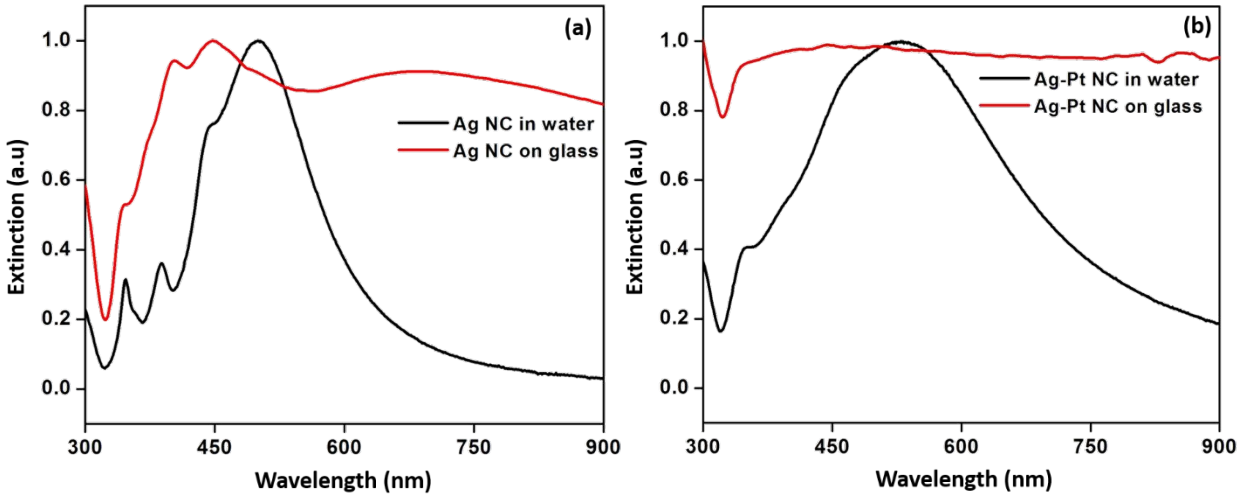

Figure S2: UV-vis extinction spectra of (a) Ag NC in water and on glass (b) Ag–Pt NC in water and on glass.

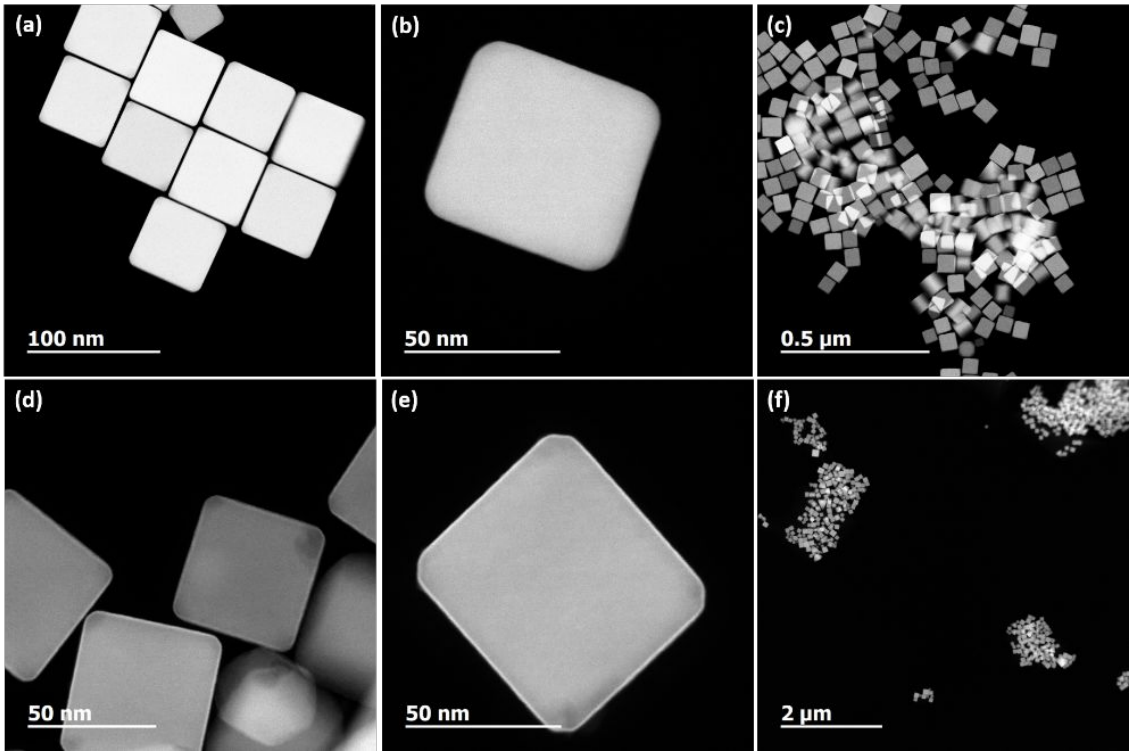

Figure S3: TEM images of Ag NC and Ag–Pt NC samples. (a), (b) TEM image of Ag nanocubes (c) TEM image of Ag nanocubes in presence of methylene blue (d), (e) TEM image of core–shell Ag–Pt nanocubes with Pt-shell thickness ~ 1.2 nm. (f) TEM image of Ag–Pt nanocubes in presence of methylene blue, methylene blue causes aggregation of nanoparticles.

For Raman (SERS) measurements we used methylene blue (MB) as a probe molecule. For the preparation of Raman samples, MB was added to aqueous colloidal solutions of Ag nanocubes or Ag–Pt nanocubes at a concentration of ~40 µM. The solution was then allowed to incubate for 3 hours to ensure full equilibrium adsorption of the dye onto the silver surface. The pH of the solution was maintained by addition of NaOH (in this manuscript wherever we mention pH we refer to the pH of the colloidal solution). Addition of MB to aqueous colloidal solution allows the molecules to access all available adsorption sites on the nanoparticles. Samples for Raman measurements were prepared by drop-casting ~40 µL of the nanoparticle–MB solution onto a cleaned silicon chip and allowing the solvent to evaporate at ~323 K, leaving behind a thin layer of nanoparticle–MB aggregates.

The wavelength dependent Raman studies were conducted using a Horiba LabRAM HR DuoScan™ system under excitation from either a 532 nm diode-pumped solid state laser or a 785 nm diode laser. The laser beam was focused onto nanoparticle aggregates with an objective microscope at a magnification of 50×. Raman scattering was detected at an angle of 180° using a Peltier-cooled (-71 ℃) charge coupled device (CCD) camera.

Higher anti-Stokes to Stokes ratio at 785-nm excitation: a consequence of charge transfer

From our SERS measurements we concluded that the measured high anti-Stokes to Stokes ratio at 785 nm excitation is the consequence of hot charge carriers transiently populating the MB molecule. However, to justify this conclusion we have corrected anti-Stokes/Stokes ratios (or intensities) for both detector sensitivity and the wavelength-dependent electromagnetic enhancements of Raman Stokes and anti-Stokes shifted photons on SERS substrates. The detailed description for the correction has been given in our earlier publications.[5,6] Briefly, for the detector sensitivity calibration, we performed Raman experiments measuring anti-Stokes and Stokes scattering intensities from a molecule (in this case liquid toluene) that exhibits no charge excitation (owing to a large HOMO-LUMO gap) and no surface Raman enhancements (liquid phase with no Ag).[6] This calibration procedure allows us to correct for the impact of the CCD detection sensitivity on our measurements through the use of a correction factor K_{CCD}, obtained by dividing the measured toluene anti-Stokes/Stokes ratio at a given Raman shift by the predicted Boltzmann ratio.[6]

The second factor responsible for deviations in the measured anti-Stokes/Stokes intensity ratio from the actual vibrational mode distribution is specific to SERS measurements (i.e., it doesn't play a role in non-surface enhanced Raman). The wavelength-dependent electromagnetic enhancements of Raman Stokes and anti-Stokes shifted photons on SERS substrates is dependent on the local value of electric field intensity at the frequencies of both the incoming and the exiting (Raman-shifted photons). The difference in frequencies of Stokes and anti-Stokes scattered photons associated with the same vibrational mode can lead to unequal electromagnetic enhancements in Stokes and anti-Stokes intensities due to unequal electric field intensities at the frequencies of Stokes and anti-Stokes scattered photons.[6,7] Briefly, we account for the electromagnetic enhancement in our measurements by considering the wavelength-dependent

Stokes and anti-Stokes spectra of probe molecules that do not undergo the charge transfer (where the electromagnetic enhancement plays the main role). We then subtract this electromagnetic-filed effect and obtain only the charge transfer effect.[5,6]

To further examine the role of charge transfer towards MB reduction and higher anti-Stokes to Stokes ratio at 785-nm excitation we employed Fe(III) as electron capturing agent (electron scavenger, we used $FeCl_3$) in Ag–Pt-MB system at pH 7. In presence of Fe(III) the Raman peaks associated with reduced form of MB does not appear with 785 nm laser excitation, and we think Fe(III) peaks up the electron before MB and in turn stops reduction of MB. Moreover, it is noteworthy that the use of Fe(III) leads to complete removal of MB anti-Stokes signal (Figure S4), which reflects on the fact that the anti-Stoke signal is indicator of direct charge transfer. To ensure the stability of nanoparticle and presence of MB on nanoparticle surface in presence of Fe(III), we collected SERS spectra using 532 nm as well as 785 nm laser light. The occurrence of SERS enhancement of Raman peaks in case of both 532 nm and 785 nm laser highlights the fact that the MB remains in the proximity of Ag-Pt NCs even in presence of Fe(III). Moreover, the Raman peak position of MB remains same at 532 nm and 785 nm (Figure S4), which suggest that there is no complexation of MB with Fe(III), which perturb MB structure.

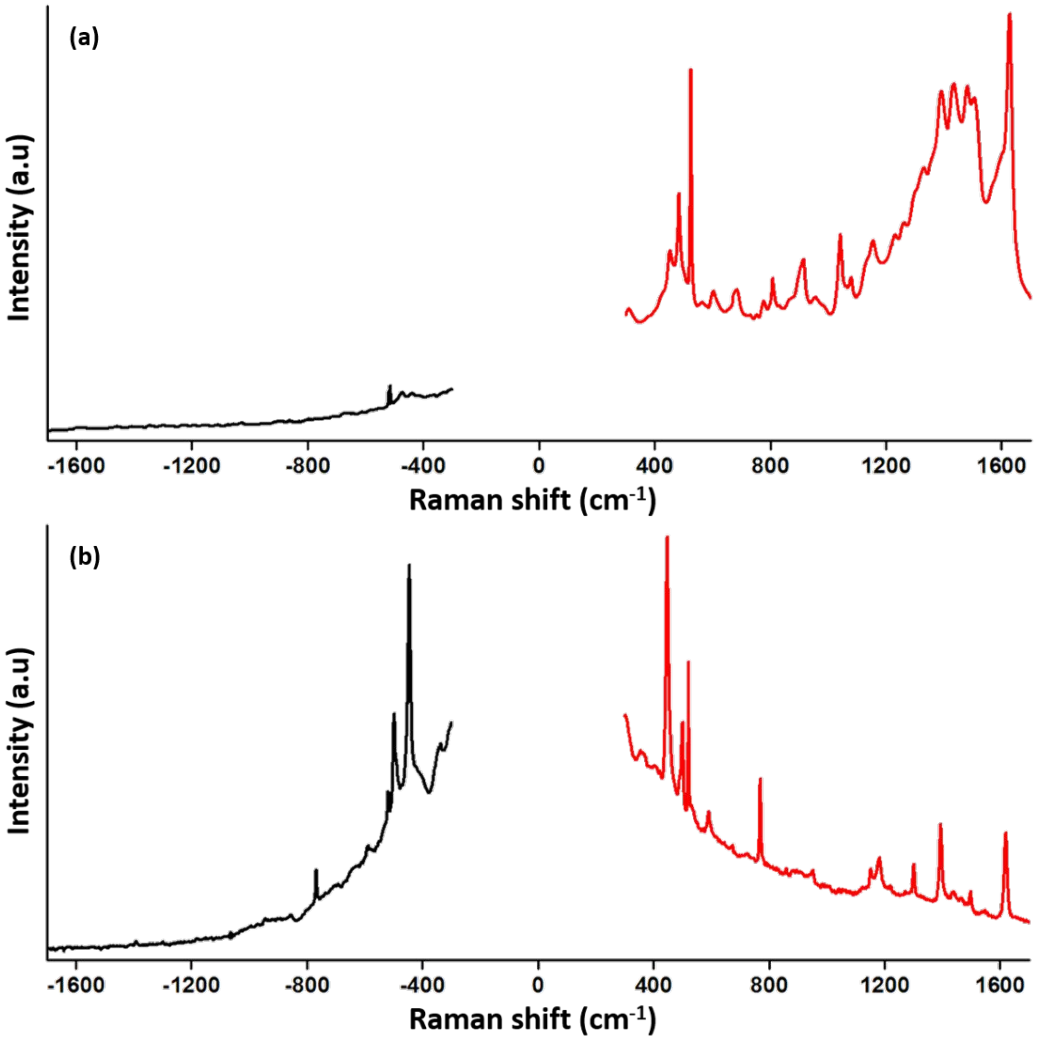

Figure S4: Surface enhanced Raman spectra (SERS) spectra showing anti-Stokes (black) and Stokes (red) spectra for Ag–Pt-MB sample in presence of $FeCl_3$ at pH 7 collected using (a) 532 nm laser and (b) 785 nm laser.

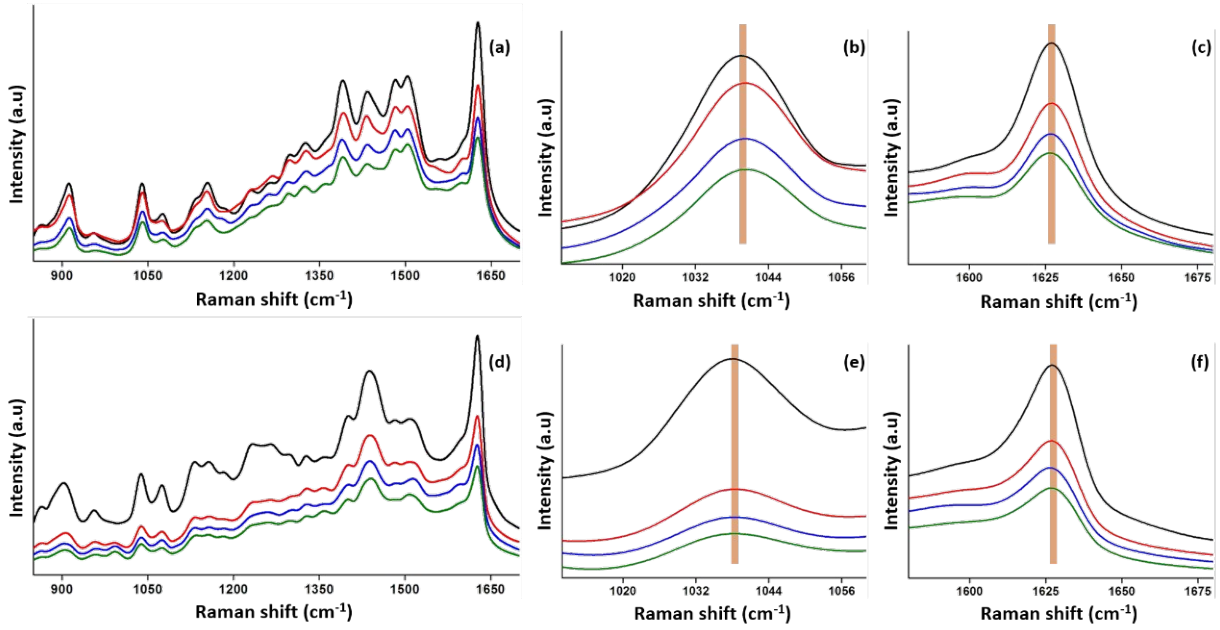

Figure S5: SERS spectra recorded to observe the direct charge transfer reaction of MB on Ag and Ag–Pt nanoparticles at pH 7 using 532 nm laser light. (a), (b), and (c) represents Stokes spectra for Ag-MB samples collected at different time interval (black: 0 min, red 2 min, blue 4 min and green 6 min). (d), (e), and (f) represents Stokes spectra for Ag–Pt-MB samples collected at different time interval (black: 0 min, red 2 min, blue 4 min and green 6 min): in each case there is no observable shift in any Raman peak with time, which suggest that the reduction of MB does not occur on either of Ag or Ag–Pt nanoparticle with 532 nm laser.

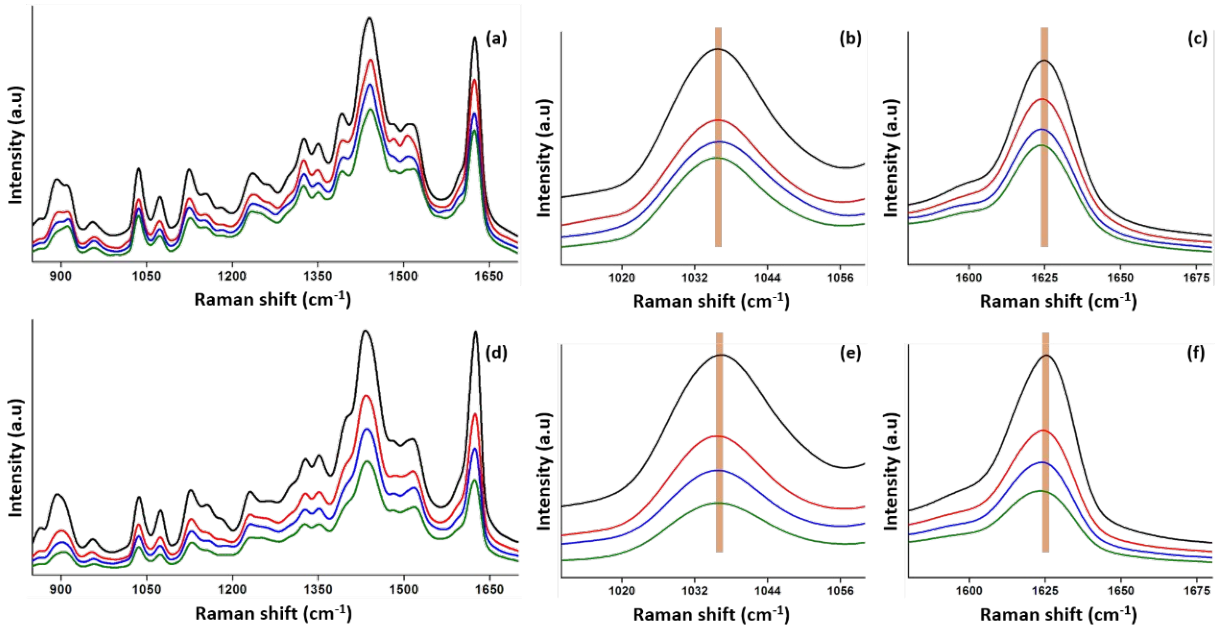

Figure S6: SERS spectra recorded to observe the direct charge transfer reaction of MB on Ag and Ag–Pt nanoparticles at pH 12 using 532 nm laser light. (a), (b), and (c) represents Stokes spectra for Ag-MB samples collected at different time interval (black: 0 min, red 2 min, blue 4 min and green 6 min). (d), (e), and (f) represents Stokes spectra for Ag–Pt-MB samples collected at different time interval (black: 0 min, red 2 min, blue 4 min and green 6 min): in each case there is no observable shift in any Raman peak with time, which suggest that the reduction of MB does not occur on either of Ag or Ag–Pt nanoparticle with 532 nm laser.

Reference:

(1) Aslam, U.; Chavez, S.; Linic, S. Controlling Energy Flow in Multimetallic Nanostructures for Plasmonic Catalysis. *Nat. Nanotechnol.* **2017**, *12* (10), 1000.

(2) Aslam, U.; Linic, S. Addressing Challenges and Scalability in the Synthesis of Thin Uniform Metal Shells on Large Metal Nanoparticle Cores: Case Study of Ag–Pt Core–Shell Nanocubes. *ACS Appl. Mater. Interfaces* **2017**, *9* (49), 43127–43132.

(3) Wang, X.; Zhang, Z.; Hartland, G. V. Electronic Dephasing in Bimetallic Gold−Silver Nanoparticles Examined by Single Particle Spectroscopy. *J. Phys. Chem. B* **2005**, *109* (43), 20324–20330.

(4) Grzelczak, M.; Pérez-Juste, J.; García de Abajo, F. J.; Liz-Marzán, L. M. Optical Properties of Platinum-Coated Gold Nanorods. *J. Phys. Chem. C* **2007**, *111* (17), 6183–6188.

(5) Boerigter, C.; Campana, R.; Morabito, M.; Linic, S. Evidence and Implications of Direct Charge Excitation as the Dominant Mechanism in Plasmon-Mediated Photocatalysis. *Nat. Commun.* **2016**, *7*, 10545.

(6) Boerigter, C.; Aslam, U.; Linic, S. Mechanism of Charge Transfer from Plasmonic Nanostructures to Chemically Attached Materials. *ACS Nano* **2016**, *10* (6), 6108–6115.

(7) Itoh, T.; Yoshida, K.; Biju, V.; Kikkawa, Y.; Ishikawa, M.; Ozaki, Y. Second Enhancement in Surface-Enhanced Resonance Raman Scattering Revealed by an Analysis of Anti-Stokes and Stokes Raman Spectra. *Phys. Rev. B* **2007**, *76* (8), 085405.